Clim Dyn (2012) 38:175–188
DOI 10.1007/s00382-010-0989-6

A multi-proxy approach for revealing recent climatic changes in the Russian Altai

Olga V. Sidorova · Matthias Saurer · Vladimir S. Myglan · Anja Eichler · Margit Schwikowski · Aleksander V. Kirdyanov · Marina V. Bryukhanova · Oksana V. Gerasimova · Ivan A. Kalugin · Andrey V. Daryin · Rolf T. W. Siegwolf

Received: 25 June 2010 / Accepted: 27 December 2010 / Published online: 8 January 2011

Abstract For the first time we present a multi-proxy data set for the Russian Altai, consisting of Siberian larch tree-ring width (TRW), latewood density (MXD), δ^{13}C and δ^{18}O in cellulose chronologies obtained for the period 1779–2007 and cell wall thickness (CWT) for 1900–2008. All of these parameters agree well between each other in the high-frequency variability, while the low-frequency climate information shows systematic differences. The correlation analysis with temperature and precipitation data from the closest weather station and gridded data revealed that annual TRW, MXD, CWT, and δ^{13}C data contain a strong summer temperature signal, while δ^{18}O in cellulose represents a mixed summer and winter temperature and precipitation signal. The temperature and precipitation reconstructions from the Belukha ice core and Teletskoe lake sediments were used to investigate the correspondence of different independent proxies. Low frequency patterns in TRW and δ^{13}C chronologies are consistent with temperature reconstructions from nearby Belukha ice core and Teletskoe lake sediments showing a pronounced warming trend in the last century. Their combination could be used for the regional temperature reconstruction. The long-term δ^{18}O trend agrees with the precipitation reconstruction from the Teletskoe lake sediment indicating more humid conditions during the twentieth century. Therefore, these two proxies could be combined for the precipitation reconstruction.

Keywords Russian Altai · Dendrochronology · Stable isotopes · Ice core · Lake sediments · Climate

O. V. Sidorova (✉) · M. Saurer · A. Eichler · M. Schwikowski · R. T. W. Siegwolf
Paul Scherrer Institute, 5232 Villigen, Switzerland
e-mail: olga.sidorova@psi.ch

O. V. Sidorova · A. V. Kirdyanov · M. V. Bryukhanova
V.N. Sukachev Institute of Forest SB RAS, Akademgorodok, 660036 Krasnoyarsk, Russia

A. Eichler · M. Schwikowski
Oeschger Centre for Climate Change Research, University of Bern, 3012 Bern, Switzerland

V. S. Myglan · O. V. Gerasimova
Siberian Federal University, Svobodniy 79, 660041 Krasnoyarsk, Russia

I. A. Kalugin · A. V. Daryin
Sobolev Institute of Geology and Mineralogy, av. Koptuga 3, 630090 Novosibirsk, Russia

1 Introduction

Valuable information about recent and past climatic and environmental changes are recorded in different natural archives such as tree-rings, ice cores, corals, historical records, lake sediments, and long instrumental observations (Jones et al. 1998; Mann et al. 1998, 2008; Bradley 1999; Mann and Jones 2003; Ammann and Wahl 2007; Robertson et al. 2009).

Annual information about climatic and environmental changes is recorded in tree-rings, ice cores, and lake sediments. A temperature signal with seasonal or weekly resolution can only be extracted from tree-ring latewood density, cell wall tree-ring chronologies and stable isotopes in tree-rings (Loader et al. 1995; Schweingruber et al. 1996; Vaganov et al. 1999, 2006; McCarroll and Loader 2004; Helle and Schleser 2004; Sidorova et al. 2010).

Trees growing at the upper tree-line in Altai are very sensitive to climatic changes and highly applicable for reconstructions of summer temperature (Loader et al. 2010).

Most of the dendroclimatic studies in this region were based on construction of tree-ring chronologies (Adamenko 1978; Ovchinnikov et al. 2002; Oidupaa et al. 2004; Panushkina et al. 2005; Myglan et al. 2008, 2009). So far, there are no latewood density, cell wall thickness, and stable isotope chronologies available. Based on previous studies from northern tree-line sites, the latewood density and cell wall thickness chronologies contain a temperature signal for the late summer (Vaganov et al. 1999; Sidorova et al. 2010).

The application of stable isotope analysis in combination with the classical dendrochronology is steadily increasing because stable isotope ratios, particularly $^{13}C/^{12}C$ and $^{18}O/^{16}O$ in wood or cellulose provide complementary information about climatic variabilities (McCarroll and Loader 2004; Saurer et al. 2002; Skomarkova et al. 2006; Gagen et al. 2006; Kirdyanov et al. 2008; Kress 2009; Sidorova et al. 2008, 2010). The $^{13}C/^{12}C$ isotopic ratio in tree-rings reflects water availability and air humidity both impacting carbon and water relations. Trees respond to limited water resources, like low amounts of precipitation and relatively warm and dry conditions with a reduction of the stomatal conductance (g_l) to prevent desiccation. Under a given photosynthetic rate low g_l values reduce the discrimination of ^{13}C against ^{12}C and increase the $^{13}C/^{12}C$ isotope ratio.

Precipitation water, which infiltrated into the soil is absorbed by tree roots and lead through the xylem vessels in the trunk to the leaves. The leaf water is then enriched in $H_2^{18}O$ because of transpiration, enhancing the oxygen isotope signal according to the climatic conditions. During photosynthesis, the oxygen of the leaf water is incorporated via carbohydrates in the biomass. Thus the $^{18}O/^{16}O$ isotopic ratios in tree-rings contain signals about temperature and precipitation, which is stored in the wood and cellulose of trees (Craig 1961; Dansgaard 1964; Saurer and Siegwolf 2007).

Therefore the carbon and oxygen isotopes measured in the same tree-rings are a useful tool for better understanding the tree responses to both, climate and climate driven changes in physiological processes. Based on this dual isotope approach it is possible to distinguish the impact of temperature or water availability (precipitation) and air humidity as the driving climatic parameter.

Ice core and lake sediments record information about long-term climatic and environmental changes with an annual up to monthly temporal resolution. The high temporal resolution in ice cores is, however, limited to upper ice core parts due to a strong thinning of annual layers with depth (Nye 1963).

Reconstructions of temperature, precipitation, and other environmental parameters from the lake sediments are based on a wide choice of lithological-geochemical proxies, which can be used for temporal calibration (Ilyashuk and Ilyshuk 2007). There are some uncertainties of sedimentary proxies because sedimentation depends on both, temperature and precipitation. Precise dating is possible only for annually laminated sediments. In addition, sedimentary records maybe affected by secondary alterations due to mineral—pore water interaction, and re-crystallization (Kalugin et al. 2007).

Each archive has its advantages and disadvantages. Climate reconstructions based on just one archive may be subject to systematic errors. For some northern areas, for instance, a divergence phenomenon has been reported between recent temperature and tree-ring trends (Briffa et al. 1998; Barber et al. 2000; Wilmking et al. 2005; D'Arrigo et al. 2008). More reliable climate reconstructions might therefore be achieved by combining different proxies because deviations between the proxies could highlight uncertainties, while common trends would indicate a high degree of reliability for the reconstruction. Despite these obvious benefits of a multi-proxy approach, few attempts have been made to explore it, apart from some large-scale reconstructions for the whole Northern hemisphere (Jones et al. 1998; Mann et al. 1998; Mann and Jones 2003; Etien et al. 2009), and apart from some multi-proxy studies within the tree-ring archive e.g. isotopes, tree-ring width and latewood density (Gagen et al. 2006; Skomarkova et al. 2006; Kirdyanov et al. 2008; Hilasvuori et al. 2009; Kress 2009). The reason for the few number of studies might be methodological challenges, like different time-resolution (annual in tree-rings, usually lower in ice-cores and lake sediments) and different seasonal information (summer in tree-rings, different seasons possible in other archives).

Temperature and precipitation reconstructions are available for the Altai Mountains from an ice core of the Belukha glacier and a sediment core from lake Teletskoe. Together with the tree-ring parameters and stable isotope chronologies, they provide an ideal setting for the application of a multi-proxy approach to reveal similarities in climate response by combining all proxies for temperature and precipitation reconstructions. To our knowledge, this is a first study, which is integrating all these independent proxies for one site. Long-term climate records are necessary to observe the development of the climate and track the impact of environmental changes on the high-altitude forest ecosystems and glaciers. However, the longest instrumental weather observations were carried out at the stations close to the cities located at much lower elevations, e.g. Barnaul (since 1834, 184 m. a.s.l.).

The goal of this paper is to provide climatic information from tree-ring parameters and stable isotopes and evaluate their suitability for temperature and precipitation reconstructions in combination with other independent proxies such as ice cores and lake sediments for tracking the climate course of the past for such a climatologically and geographically complex region as the Russian Altai.

2 Materials and methods

2.1 Study site of the tree-ring parameters

The study area is located in the vast Altai-Sayan Mountain region, in the Tuva Republic of the Russian Federation in southern Siberia, the central part of the north Asian continent. It is characterized by a complex geophysical relief. The Altai-Sayan eco-region is a mosaic of coniferous forests, intermontane steppes, and alpine meadows.

Tree-ring material was collected from living *Larix sibirica* Ldb. trees growing in the Mongun taiga, Tuva Republic, Russia [50° 23′ N, 89° 04′ E] (Fig. 1a, b). This region is isolated from industrial centers.

The sampled trees were growing at elevations of 2280–2340 m a.s.l., which is in the range of the current position of the upper treeline (2,250–2,400 m a.s.l.). The age of trees can exceed 600 years at this location (Fig. 1c). Four to six cores were taken from each tree at a height of 1.3 m with a 0.5-cm-diameter increment borer. The cores were used for tree-ring width, latewood density, cell wall structure, and stable isotope measurements.

The study site is covered by permafrost with a maximal thawing depth of 80–100 cm. The snow melt starts at the end of May or early June and the first snow falls in the middle of August–September, considerably varying from year to year.

2.2 Climate

The study site is characterized by a continental climate. The duration of the vegetation season with summer temperatures above 10°C at an altitude of 1,400 m is around 80 days (Sevastyanov 1998). The precipitation amount at the study site is about 170–220 mm per year.

The present-day climate is largely controlled by the Siberian-Mongolian high atmospheric pressure zone, along with westerly low-pressure systems linked to the North Atlantic influence (Efimtsev 1958; Alpatev et al. 1976; Ilyashuk and Ilyshuk 2007). Atmospheric circulation has a seasonal pattern in the study region. The Siberian-Mongolian

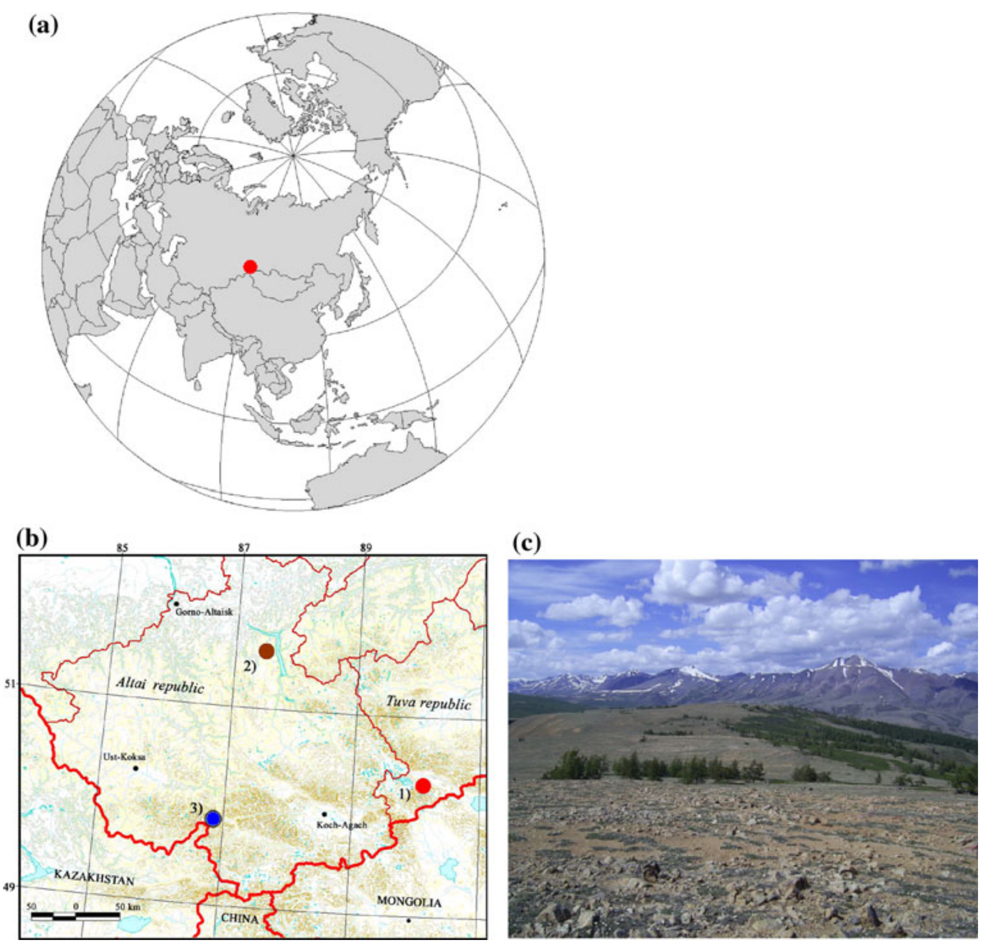

Fig. 1 Maps with **a** the location of the study region (*red dot*), **b** the sampling site in the Tuva Republic, Russia (*1-red dot*); Teletskoe lake (*2-brown dot*), and Belukha glacier (*3-blue dot*) and **c** photo of the sampling site (Photo by V.S. Myglan)

anticyclone centered in the Tuva basin and northern Mongolia is dominant from early October–November until April (Sevastyanov 1998). Westerlies are prevalent in summer, with air masses coming from Kazakhstan and in autumn bringing strong winds and rain. The temperature inversion becomes important in November, when the temperature decreases to −30°C.

The availability of weather station data close to the study site is limited due to the length of the observation period and gaps in the data. Monthly temperature and precipitation data were available for the weather stations from Russian Altai: Kosch-Agach (50° 02′ N, 88° 68′ E, 1,758 m. a.s.l.); Ak-kem (49° 55′ N, 86° 32′ E, 2,056 m. a.s.l.); Barnaul (53° 43′ N, 83° 52′ E, 184 m. a.s.l.), Mongolian Altai, Ulgii (48° 93′ N, 89° 93′ E, 1,715 m a.s.l.); and from Chinese Altai (47° 73′ N, 88° 08′ E, 737 m. a.s.l.) http://climexp.knmi.nl. The summer temperature trends are similar between the different weather stations, while the precipitation records show different patterns. This is due to strong regional differences in precipitation deposition and re-distribution in mountain areas. We chose the weather data from Kosh-Agach station for statistical analyses, since this is the closest high-altitude station within 104 km from the sampled site. Monthly data for precipitation and temperature were available for the period 1934–1993 and 1961–1995, respectively. Gridded temperature and precipitation data (0.5° × 0.5°) for the period from 1901 to 2005 were used for spatial correlation analysis with tree-ring parameters and δ^{13}C, and δ^{18}O in tree-ring cellulose within the coordinates 45° N–55° N and 70° E–100° E from 1901 to 2005 http://climexp.knmi.nl (CRU version TS3).

2.3 Tree-ring width (TRW), maximum latewood density (MXD) and cell wall thickness (CWT) chronologies

The tree cores were measured using the semi-automatic devices LINTAB V-3.0 (Rinn Tech GmbH, Germany) with a precision of 0.01 mm and cross-dated for determining the exact calendar date for each tree-ring (Schweingruber et al. 1996; Cook and Krusic 2008). The individual tree-ring width series were standardized using a negative exponential curve or linear regression to remove age-related trends. The absolutely dated standardized site chronology was constructed by using 20 individual tree series within the 400–500-year age class.

Tree-ring density was measured using the densitometer DENDRO-2003 at the V.N. Sukachev Institute of Forest, SB RAS, Krasnoyarsk, Russia according to the method described by Schweingruber (1996). To construct the master MXD chronology, each of the individual series was standardized using the cubic smoothing splines with 50% frequency–response cutoff equal to 2/3 of the series length. Data for 23 living trees were used to construct a maximum latewood density chronology.

The Expressed Population Signal (EPS) was calculated to define a threshold level of common signal between tree-ring series in year-to-year variations, i.e. the sensitivity of the tree-ring width variability to changes of external factors, which is based on the average correlation between the trees. The EPS higher or equal 0.85 is considered to be reliable along its whole length (Wigley et al. 1984; Cook and Kairiukstis 1990).

Hamming smoothing (Blackman and Tukey 1958) with 41-year window (Esper et al. 2002) was used for revealing long-term trends for all chronologies.

Cell structure of tree-rings was measured for 5 trees for the period 1900–2007 with an Image analysis system (AxioVision) (Carl Zeiss, Germany) at the V.N. Sukachev Institute of Forest SB RAS. Cell wall thickness was determined in five radial series of cells from the outside border in each tree-ring to the inside border. Measurements of double cell wall thickness in the radial direction, lumen diameter, and hence cell sizes were made along each radial file sampled. The resolution and precision of measurements were approximately 0.3 µm.

Since tree-ring width and, consequently, the number of tracheids varies between different years, the measurements were normalized to a standard number of cells (Vaganov et al. 2006).

2.4 δ^{13}C and δ^{18}O in tree-ring cellulose

Of the cross-dated samples we selected core samples from the five trees for the recent period for the analyses of ^{13}C/^{12}C and ^{18}O/^{16}O isotope ratios in tree-rings based on similar tree-ring width patterns. The first 50 years of each sample were not considered to exclude the influence of the juvenile effect (McCarroll and Loader 2004; Gagen et al. 2008; Sidorova et al. 2008, 2009).

The ^{13}C/^{12}C and ^{18}O/^{16}O isotope ratios were analyzed separately for each single tree for the period 1779–2007. After splitting the rings with a razor knife, the whole wood samples were enclosed in filter bags and cellulose extraction was performed according to the method described by Loader et al. (1997) and Boettger et al. (2007). Due to a low amount of the cellulose material some of the δ^{18}O values could not be determined.

0.2–0.3 mg of cellulose for each annual ring was weighed into tin capsules for the analysis of the ^{13}C/^{12}C and 0.5–0.6 mg into silver capsules for the of ^{18}O/^{16}O ratio.

The carbon and oxygen isotopic ratios in cellulose were determined with an isotope ratio mass spectrometer delta-S (Finnigan MAT, Bremen, Germany) linked to two elemental analyzers (EA-1108, and EA-1110 Carlo Erba, Italy) via a variable open split interface (CONFLO-II, Finnigan MAT, Bremen, Germany) at the stable isotope facility of the Paul Scherrer Institute, Villigen, Switzerland. $^{13}C/^{12}C$ was determined by combustion under excess oxygen at a reactor temperature of 1,020°C, while samples for $^{18}O/^{16}O$ ratio measurements were pyrolyzed to CO at 1,080°C (Saurer et al. 1998), both operating in the continuous flow mode. This guarantees a high sample throughput rate with a good precision for $\delta^{13}C$ ($\sigma \pm 0.1$‰) and $\delta^{18}O$ ($\sigma \pm 0.2$‰). The precision is based on a large number of measurements of the standard material and quality control (N > 100). The isotopic values were expressed in the delta notation relative to the international standards:

$$\delta_{\text{sample}} = (R_{\text{sample}}/R_{\text{standard}} - 1) \times 1,000,$$

where R_{sample} is the molar fraction of $^{13}C/^{12}C$, or $^{18}O/^{16}O$ ratio of the sample and R_{standard}, of the standards of Vienna Pee Dee Belemnite (VPDB) for carbon and Vienna Standard Mean Ocean Water (VSMOW) for oxygen.

2.5 ^{13}C correction

Changes in the atmospheric CO_2 isotope composition are directly reflected in the isotopic ratios of the photosynthesis products. We calculated the differences between each year and the pre-industrial value (1850) for $\delta^{13}C$ of atmospheric CO_2 obtained from ice cores and direct atmospheric measurements at the Mauna Loa Observatory, Hawaii (Francey et al. 1999 http://www.esrl.noaa.gov/gmd/ccgg/globalview/co2c13/co2c13_intro.html) and subtracted the differences from the raw carbon isotope series for each year. Because the isotope fractionation is additive, this completely removes the trend of decreasing isotopic composition in the atmosphere resulting from the combustion of fossil fuel emissions and land use change.

A pre-industrial 'pin' correction, taking into account the changes in the active response of trees to the increased availability of CO_2 by increasing their water use efficiency was additionally applied (McCarroll et al. 2009). This correction was successfully applied for the $\delta^{13}C$ chronologies from high latitude sites already (Sidorova et al. 2009, 2010). The pin-correction results in improved correlations between climate data and carbon isotope series, because the non-climatic direct CO_2-effects on plant physiology are removed. For further analysis and discussions we will therefore only use the two-fold corrected $\delta^{13}C$ chronology.

2.6 Ice core and lake sediment data

To compare the tree-ring records with independent climate proxies, we used published reconstructed temperature and precipitation ice core data from the Belukha glacier (49°48′ N, 86° 34′ E, 4,062 m. a.s.l.) (Henderson et al. 2006; Eichler et al. 2009) and reconstructed temperature and precipitation data from Teletskoe lake sediments (51° 39′, 87° N 40′ E, 434 m asl) (Kalugin et al. 2007). Both sites are located within 200–300 km from each other as well as from the dendrochronological study site (Fig. 1b).

The ice core drilling site was at the glacier saddle between Belukha east and west summit, the highest mountains of the Altai. The main precipitation season at this site is between March and November. The 139 m ice core covers the time period 1250–2001 (Eichler et al. 2009), which was established by annual layer counting, ^{210}Pb dating, identification of volcanic horizons, and the use of a kinematic glacier flow model. Dating uncertainty is up to 3 years for the investigated time period 1779–2000 in this study.

The ice core $\delta^{18}O$ record was found to be a good high-resolution March-November temperature proxy for the last 750 years. This was based on the correlation between 10-year averaged $\delta^{18}O$ values and Barnaul temperatures r = 0.83; r < 0.05 for the instrumental period 1850–1980.

Reconstructed temperatures are highly correlated with solar activity proxies for the period 1250–1850, revealing high (low) values during periods of high (low) solar activity. After 1850 a strong temperature increase was observed, correlated with the increasing CO_2 emissions for the period 1850–2000 (Eichler et al. 2009). Temporal changes in ice core melt percentages have been successfully applied as summer (June–August) temperature proxy for the period 1818–2001 (Henderson et al. 2006). The correlation coefficient between 10-year averaged temperature based on melt percentages and Barnaul June–August temperature was $r = 0.82$; $P < 0.05$ for the period 1850–1999. The two temperature proxies indicate a strong warming trend of about 2°C in the last 150 years in the continental Siberian Altai.

The reconstructed accumulation obtained from the record of annual layers thickness of the Belukha ice core was used as a precipitation proxy for the period 1818–2001 (Henderson et al. 2006). No trend was found in this period, except for the precipitation maxima around 1830 and 1950.

Teletskoe lake is located in the taiga zone of the north-eastern Altai region (51° 39′ N, 87° 40′ E, 434 m a.s.l.). The lake accumulates sediments continually. More than half of the water input to the lake is provided by spring and summer floods after the seasonal snow melt. Generally, the climate in the lake region is continental (Selegei et al. 2001); the influence of the Siberian High prevails in winter, and westerly influence increases in summer.

Sediment cores from the Teletskoe Lake were collected from the deepest area at a water depth of 325 m. They were analysed by X-ray fluorescence with synchrotron radiation

(XRF-SR) with an increment step of 0.2 mm corresponding to a unique resolution of 2–3 months. The composition and physical properties of the sediments were studied by standard procedures with discrete sub-sampling at 0.5 cm resolution.

Dating was performed by gamma spectrometry of ^{137}Cs and ^{210}Pb for the uppermost 10 cm as well as ^{14}C measurements for lower layers of core. Both methods showed the same accumulation rate of about 0.9 mm/year which was accepted for the wet sediment (Kalugin et al. 2007).

Annual environmental reconstruction by Teletskoye lake sediments is based on linear age model which has not provided exact dating like tree ring series because layers thickness varies year by year. The position of the peaks could be displaced on absolute time scale. That allows comparing with other proxies only for lower frequency environmental oscillations—ca 5 years and longer. This problem would be corrected by fitting of peaks on well-known events or by study of annually laminated sediments.

To reconstruct temperatures, the time series of X-ray density (XRD) of the sediment, the Sr/Rb ratio, and the contents of Br were used (Kalugin et al. 2007). The function of T = f (Br, XRD, Sr/Rb) was calibrated using the data from the Barnaul weather station. The correlation coefficients between smoothed by 25-year window averaged annual temperature from the Barnaul weather station data and Sr/Rb, Br, XRD were ($r = 0.71$; $r = 0.87$ and $r = -0.84$; $P < 0.05$), respectively, for the period 1840–1991. The correlation coefficients between smoothed by 25-year window averaged annual precipitation from the Barnaul weather station data and Sr/Rb, Br, XRD were ($r = -0.37$, $r = -0.83$, $r = 0.60$; $P < 0.01$) for the period 1880–1991.

The paleotemperature reconstruction obtained for the last two millennia indicate the similar values of recent warming. Negative significant correlation between the flood lake level and temperature was observed for the period between AD 1930 and 1996. Taking into account modern warming, this level was explained by extra-melting of perennial snow in high mountains against a background of aridization trend.

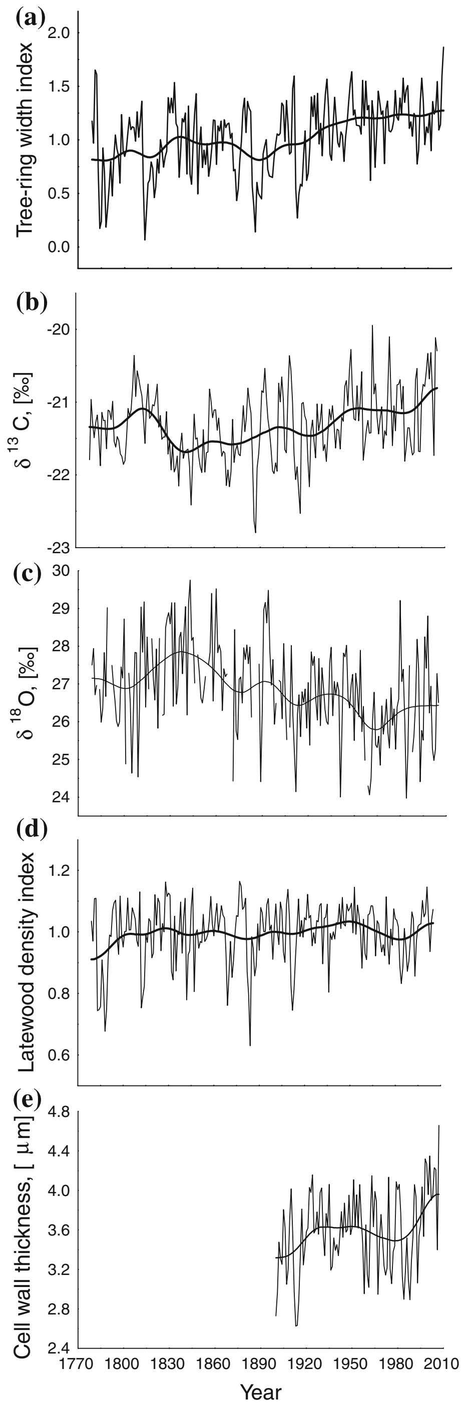

Fig. 2 Annual and smoothed chronologies of tree-ring width (**a**), $\delta^{13}C$ in cellulose (**b**), $\delta^{18}O$ in cellulose (**c**), latewood density (**d**), and cell wall thickness (**e**) are shown. The smoothing was performed by using a 41-year Hamming window

3 Results

3.1 TRW, MXD, CWT, $\delta^{13}C$ and $\delta^{18}O$ of cellulose chronologies

TRW, MXD, $\delta^{13}C$, and $\delta^{18}O$ in cellulose chronologies were obtained for the period 1779–2007, while CWT was constructed for the period 1900–2007 (Fig. 2a–e).

The EPS is very high on both, tree-ring width (0.94–0.97) and latewood density (0.91–0.96) chronologies for the period of 1779–2007. Based on significant correlations between the chronologies from five individual trees for carbon ($r = 0.70$–0.80; $P < 0.05$) and for oxygen ($r = 0.53$–0.70; $P < 0.05$) and high EPS values 0.87 for carbon and 0.85 for oxygen the average chronologies for

Table 1 Correlation coefficients between (a) annual and (b) smoothed chronologies of TRW, MXD, CWT, δ^{13}C and δ^{18}O of cellulose

	δ^{13}C	δ^{18}O	TRW	MXD	CWT
(a)					
δ^{13}C	1				
δ^{18}O	**0.15**	1			
TRW	**0.26**	0.01	1		
MXD	**0.23**	**0.19**	**0.66**	1	
CWT	**0.59**	**0.43**	**0.55**	**0.67**	1
(b)					
δ^{13}C	1				
δ^{18}O	**−0.65**	1			
TRW	0.57	**−0.64**	1		
MXD	0.25	−0.21	0.56	1	
CWT	0.67	−0.03	**0.71**	0.55	1

The smoothing was performed by using a 41-year Hamming window

The significant coefficients at the 95% level are in bold

The annual and smoothed data for TRW, MXD, δ^{13}C and δ^{18}O of cellulose chronologies for the period 1779–2005 and CWT chronologies for the period 1900–2005 are presented

δ^{13}C (Fig. 2b) and δ^{18}O (Fig. 2c) in cellulose were constructed.

TRW (Fig. 2a), δ^{13}C (Fig. 2b), and CWT (Fig 2e) chronologies show an increasing trend in the last 120 years. The δ^{18}O cellulose chronology (Fig. 2c) shows a steadily declining trend in the last 150 years, whereas there is no long-term trend in the MXD chronology (Fig. 2d).

Correlation analyses were performed for the annual values (Table 1a) and smoothed data (Table 1b) to obtain information on both, short-term variations and the long-term trend, respectively. In general, all chronologies are significantly positively correlated in year-to-year variability between each other. The correlation coefficients between δ^{18}O in cellulose in comparison with the other records are lowest. The smoothed δ^{18}O cellulose chronology is negatively correlated with δ^{13}C in cellulose for the period 1779–2005 (Table 1b), opposite to the year-to-year variability, which is positively correlated (Table 1a).

3.2 High-frequency variability in TRW, MXD, CWT, and δ^{13}C, δ^{18}O of cellulose and climatic parameters

Significant correlations are obtained between TRW, MXD, CWT, and temperatures of June and July (Fig. 3a–c), δ^{13}C of cellulose and July temperature (Fig. 3d), and δ^{18}O and temperatures of January, March, May, July, and August (Fig. 3e).

The comparison with precipitation data reveals a positive significant correlation between MXD and March precipitation (Fig. 3g), and δ^{13}C and April precipitation (Fig. 3i). Negative correlation coefficients were found between July precipitation and δ^{13}C and δ^{18}O of cellulose chronologies (Fig. 3i, j). A negative significant correlation was also found between January precipitation and δ^{18}O of cellulose (Fig. 3j).

In summary, results of the correlation analysis between tree-ring parameters, stable isotopes chronologies and weather station data indicate that information about July temperature is recorded in all studied parameters (e.g. July temperature and TRW ($r = 0.63$; $P < 0.05$); MXD ($r = 0.54$; $P < 0.05$); CWT ($r = 0.63$; $P < 0.05$), δ^{13}C ($r = 0.62$; $P < 0.05$) and δ^{18}O ($r = 0.50$; $P < 0.05$) chronologies (Fig. 3a–e).

The July precipitation signal is recorded only in δ^{13}C ($r = -0.41$; $P < 0.05$) and δ^{18}O ($r = -0.32$; $P < 0.05$) of cellulose chronologies (Fig. 3i, j). Due to the importance of July, the spatial dimension of the correlation coefficients between all the studied chronologies and July temperature and precipitation for all available gridded data sets were calculated to get the patterns of climate change for the period from 1901 to 2005 (Fig. 4).

The correlation coefficients calculated based on gridded July temperature showed the strongest spatial distribution in MXD (Fig. 4b) and CWT (Fig. 4c). There is no spatial correlation between TRW and July precipitation (Fig. 4f, right panel), while MXD, δ^{13}C and δ^{18}O of cellulose chronologies show a significant correlation with July precipitation (Fig. 4g–j, right panel).

3.3 Long-term temperature signal in TRW, MXD, CWT, δ^{13}C and δ^{18}O in cellulose chronologies

Based on the correlation analyses for monthly climate data, spatial distribution of the correlations for gridded July air temperature data, and annual tree-ring parameters and stable isotope values we conclude that short-term (annual) variations in TRW, MXD, CWT, and δ^{13}C of cellulose chronologies record a strong July temperature signal. To evaluate the low-frequency behavior of the proxies, correlation analyses between smoothed temperature reconstructions from the Belukha ice core and Teletskoe lake sediments were carried out (Eichler et al. 2009, Kalugin et al. 2007) (Fig. 5a, Table 2). TRW and δ^{13}C of cellulose are highly correlated with temperature reconstructions obtained from the Belukha (δ^{18}O ICE, MT) and Teletskoe site (TSED), while there are no significant correlations with MXD and CWT (Table 2). This is due to the strong decrease in the MXD and CWT records around 1980, not observed in the other chronologies. Thus, only TRW and δ^{13}C reflect temperature in the long-term trend, revealing a

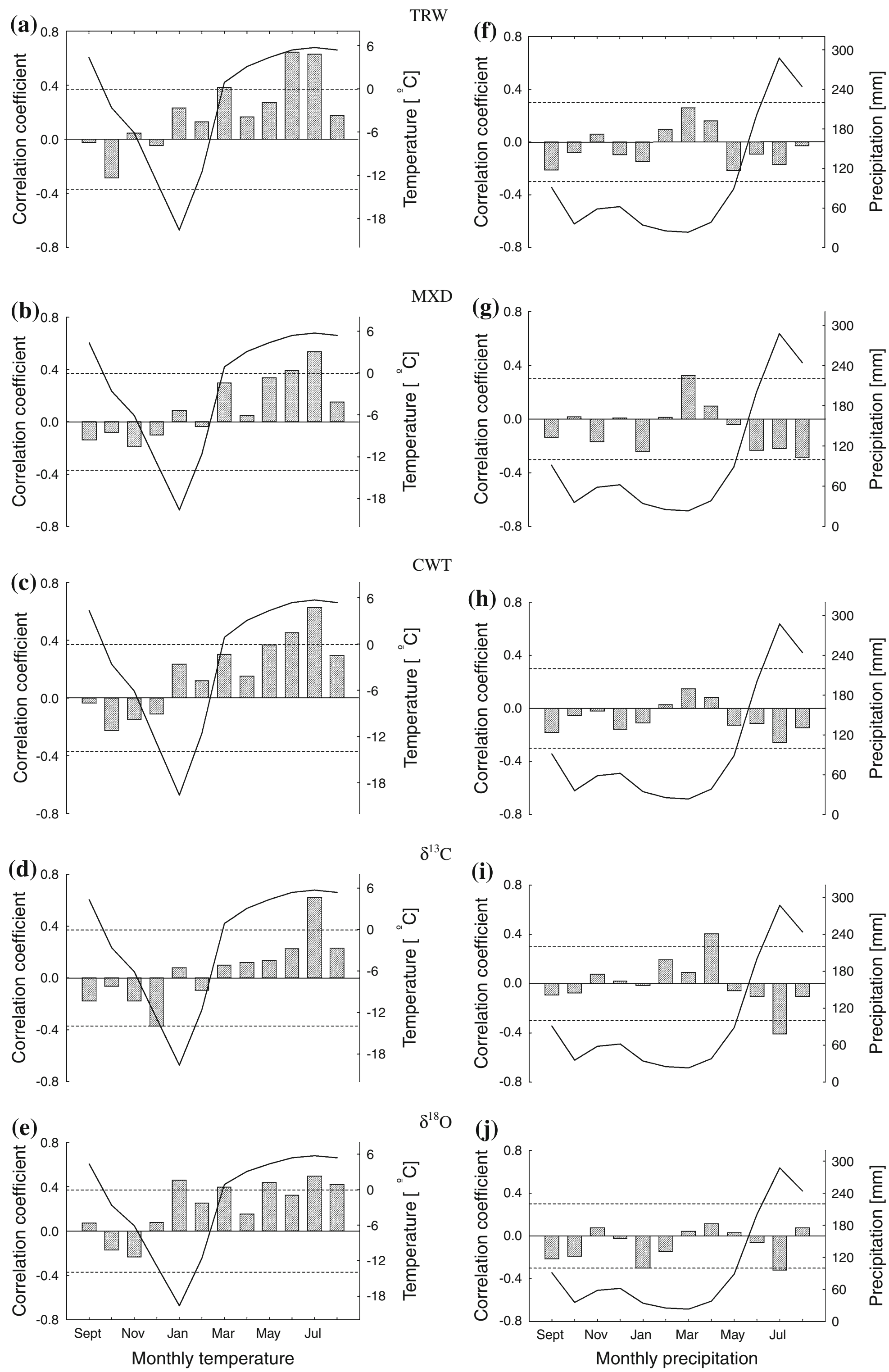

Fig. 3 The correlation coefficients between annual values of tree-ring width (TRW), latewood density (MXD), cell wall thickness (CWT), δ^{13}C and δ^{18}O in cellulose and temperature (**a–e**) (1958–1993), and precipitation (**f–j**) (1934–1993) calculated for the high-altitude Kosh-Agach weather station from September of the previous year to August of the current year. The horizontal lines indicate the level of significance ($P < 0.05$). The monthly temperatures and precipitations data from Kosh-Agach weather station are shown as a *bold line* curves on the graphs (**a–e**) and (**f–j**), respectively

pronounced increase after 1880 (Fig. 5b). We found highly negative significant correlations between δ^{18}O of cellulose and δ^{18}O ICE, MT, TSED, TRW and δ^{13}C of cellulose (Table 2, Fig. 5a) in long-term variations, in spite of the fact that short-term signals are positively related.

3.4 Long-term precipitation signal in MXD, δ^{18}O and δ^{13}C of cellulose chronologies

Based on the correlation analyses between annual tree-ring parameters, stable isotope values and July precipitation

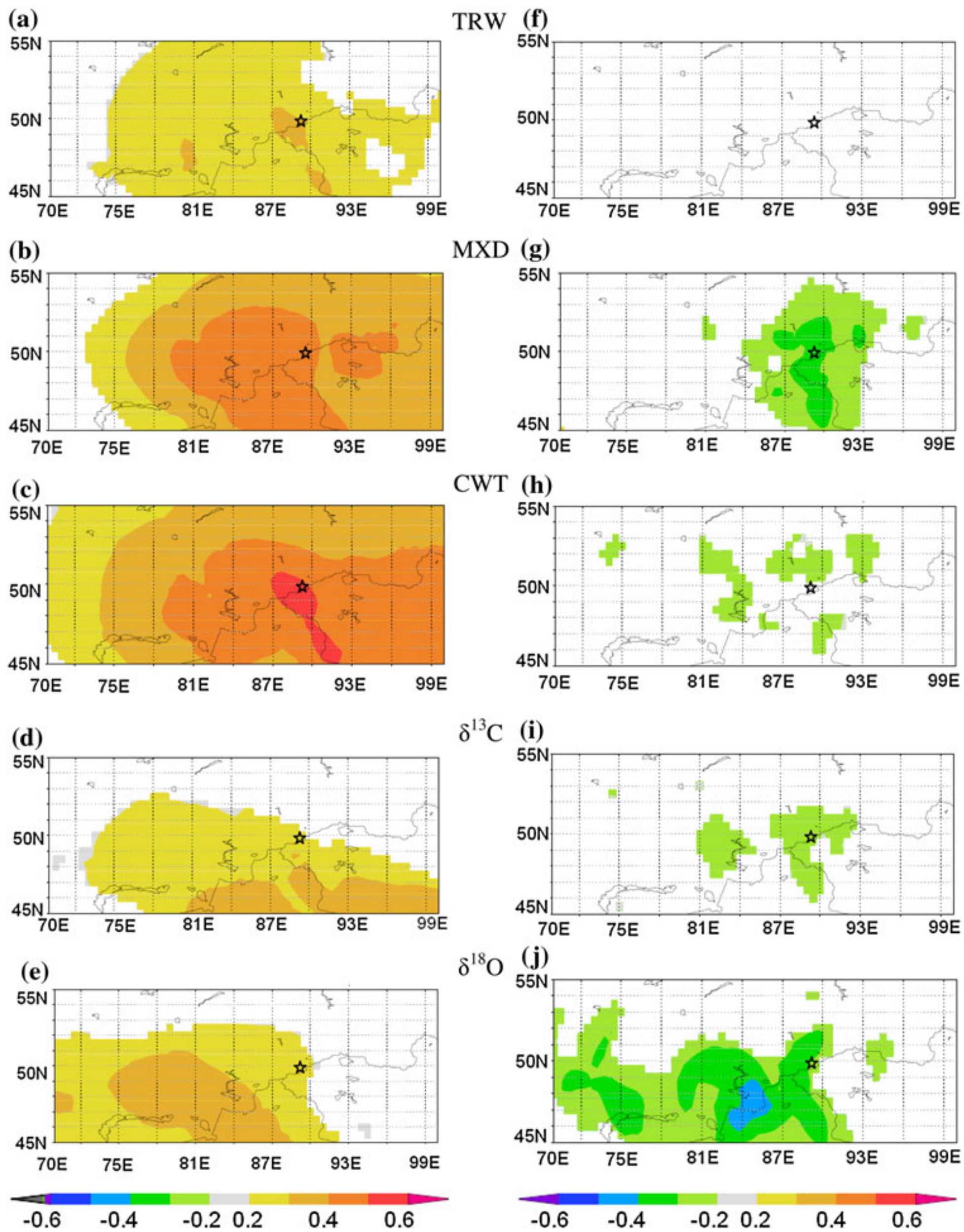

Fig. 4 Spatial distribution of correlation coefficients between TRW, MXD, CWT, δ^{13}C, δ^{18}O, and gridded July temperature data (*left panel*, **a–e**) (http://climexp.knmi.nl) and July precipitation (*right panel*, **f–j**) (http://climexp.knmi.nl) with a spatial resolution up to 2.1° × 0.5°, $P < 5\%$ for the period between 1901 and 2005. The colors indicate the correlations, negative correlations are represented by blue to *green* colors, whereas positive correlations are represented by red to *yellow* colors (see the color scales at the bottom of the figures panels). The *asterisks* indicate the study site

from the local weather station data and the spatial patterns we found that a precipitation signal is recorded in short-term variations of δ^{18}O, δ^{13}C, and MXD chronologies.

The comparison between smoothed chronologies of δ^{18}O, δ^{13}C of cellulose, MXD and precipitation reconstructions from Teletskoe lake sediments (Kalugin et al. 2007) and from Belukha ice core (Henderson et al. 2006) are shown in Fig. 6a (PSED, AP). The correlation coefficients calculated between all these proxies showed that for the common period from 1818 to 2000 in the long-term fluctuations only δ^{18}O of cellulose chronology correlated significantly with the precipitation reconstruction from Teletskoe lake (Table 2). For the comparison with the precipitation record derived from lake sediments we inverted the δ^{18}O of the cellulose chronology from negative to positive values, to account for the negative correlation with precipitation (Fig. 6b). The chronologies show similar long-term trends during the study period, with a pronounced increase since the middle of the nineteenth century.

4 Discussion

4.1 Short-term variations in tree-ring parameters and stable isotopes

A multi-proxy data set consisting of tree ring width, latewood density, cell wall thickness, δ^{13}C and δ^{18}O in

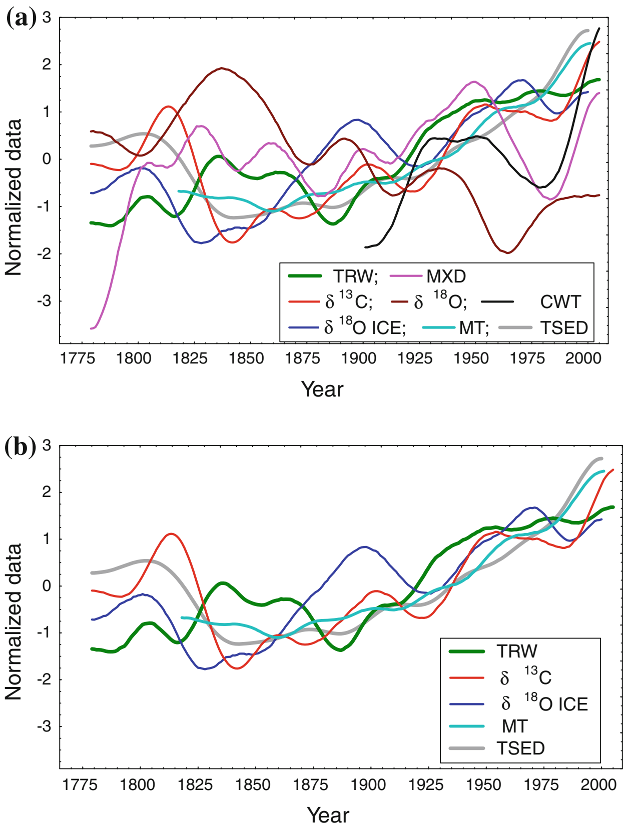

Fig. 5 Normalized smoothed by 41-year Hamming window chronologies of **a** TRW, MXD, CWT, δ^{13}C, and δ^{18}O significantly correlated with gridded July temperature in year-to year variability and **b** TRW, and δ^{13}C significantly correlated in low-frequency variability with temperature reconstructions obtained from δ^{18}O in the Belukha ice core (δ^{18}O ICE), from the percent melt values from Belukha ice core (MT), and from Teletskoe lake sediments (TSED)

cellulose chronologies have been obtained for the Altai-Sayan region.

The correlation analysis showed positive significant relationships between July air temperature and tree-ring parameters and stable carbon isotope values resulting from an increasing photosynthetic rate (because this leads to lower intercellular CO_2-concentration in the leaf, lower isotope discrimination and more positive δ^{13}C values in the plant organic matter (Farquhar et al. 1989). The negative correlations of δ^{13}C in cellulose with July precipitations on the other hand can be explained by reduced stomatal conductance due to drought conditions, since July is the warmest month. The positive correlations with January temperature and the negative correlation with January and July precipitation were observed only for δ^{18}O in cellulose that could be explained by changes in the atmospheric circulation patterns and the seasonality of the precipitation. Snowfall in winter can influence δ^{18}O of tree-rings via water storage and melting in spring. A similarly weaker response between δ^{18}O in cellulose and temperature compared to δ^{13}C in cellulose was detected for the high latitude sites in northeastern Yakutia (Sidorova et al. 2008), eastern Taimyr (Sidorova et al. 2010), central Tura (Sidorova et al. 2009), and northern Finland (Hilasvuori, 2009). While MXD was mainly influenced by summer conditions, a positive correlation between MXD and March was found. It could be explained by similar trends between both parameters and exceptional conditions during March of the year 1953, which is characterized by high precipitation amounts (186 mm), exceeding the average value by three times. No significant relationships between TRW, CWT

Table 2 Correlation coefficients between proxies which are smoothed by 41-year Hamming window

	PSED	δ^{18}O	AP	MXD	δ^{13}C	TRW	CWT	TSED	δ^{18}O ICE	MT
PSED	1									
δ^{18}O	**−0.81**	1								
AP	−0.34	0.09	1							
MXD	0.24	−0.20	0.43	1						
δ^{13}C	0.30	**−0.66**	0.15	0.19	1					
TRW	0.54	**−0.63**	0.12	0.54	0.53	1				
CWT	0.47	−0.07	0.26	0.55	0.56	**0.72**	1			
TSED	0.31	**−0.65**	−0.06	−0.03	**0.89**	**0.60**	0.52	1		
δ^{18}O ICE	**0.84**	**−0.92**	−0.17	0.17	**0.68**	**0.60**	0.16	**0.65**	1	
MT	0.52	**−0.73**	−0.03	0.18	**0.89**	**0.86**	0.56	**0.98**	**0.77**	1

The significant coefficients at the 95% level are in bold

Temperature reconstruction from melt percent index from Belukha ice core (MT) and precipitation reconstruction from accumulation of precipitation in Belukha ice core (AP) for the period (1818–2000)

Cell wall thickness chronology (CWT) for the period (1900–2000)

Tree-ring width (TRW), latewood density (MXD), δ^{13}C of cellulose (δ^{13}C), δ^{18}O in cellulose (δ^{18}O), temperature (TSED) and precipitation (PSED) reconstructions from Teletskoe lake sediments, temperature reconstructions from δ^{18}O in Belukha ice core (δ^{18}O ICE) (1779–2000)

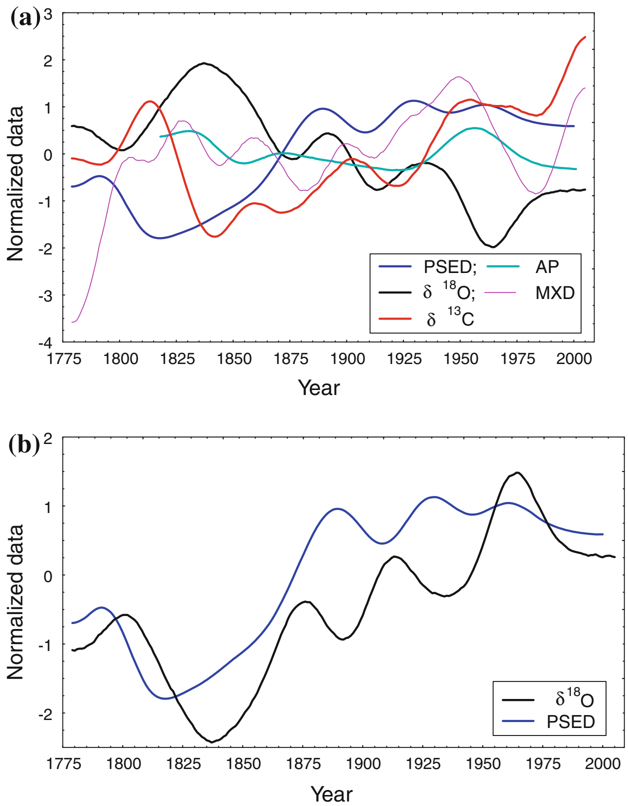

Fig. 6 Normalized smoothed by 41-year Hamming window chronologies of **a** MXD, δ^{13}C, and δ^{18}O (significantly correlated with gridded July precipitation in year-to year variability) compared to precipitation reconstruction from the Teletskoe lake sediments (PSED) and precipitation reconstruction from Belukha ice core (AP) and **b** δ^{18}O of cellulose and precipitation reconstruction from Teletskoe lake sediments (PSED) chronologies, which are correlated in long-term variations

and monthly precipitation chronologies were found. A spatial correlation between the annual tree-ring parameter and temperature/precipitation also clearly demonstrates a stronger influence of temperature on the TRW, MXD, CWT, δ^{13}C in cellulose, whereas δ^{18}O of cellulose shows a mixed signal.

Annual chronologies of MXD, δ^{13}C, and δ^{18}O are anti-correlated with precipitation data from the closest high-altitude station. However, δ^{18}O is the only parameter of the three revealing a stronger spatial correlation with precipitation than with temperature. Not surprisingly and due to limited numbers of the high elevated weather station data, short periods of observations and gaps in the data sets, the spatial correlations are lower for precipitation than for temperature (Fig. 4). Such data sets are hard to use for the calibration and verification models, which are used to produce a reconstruction for precipitation. The differences in the elevation and air inversions should be taken into account as well. The weather stations, which are located in the valley at low altitudes, could show completely different amounts of precipitation compared to the study site, which is located at more than 2000 m a.s.l. In this case multiple approaches with other natural archives will help to reduce the uncertainties of further possible precipitation reconstructions for the study region.

4.2 Long-term variations in temperature proxy records

A pronounced increasing trend since the 1880s was found for the TRW, and δ^{13}C chronologies indicating an air temperature increase. This strong increase is also clearly reflected in the lake sediment and ice core temperature reconstructions (δ^{18}O ICE, MT) and was explained by the rising anthropogenic CO_2 emissions in the industrial period (Eichler et al. 2009). Additionally, similar to the temperature reconstruction from δ^{18}O in the ice core, the δ^{13}C in tree cellulose shows two pronounced minima around 1840 and 1920, explained by temperature minima during periods of decreased solar activity (Dalton, Gleissberg minima).

The high correlations between the smoothed TRW and δ^{13}C of cellulose chronologies and the temperature proxies indicate similar trends for decadal-scale and longer-term variability. The weaker correlations with CWT and the missing correlation with the MXD in long-term variations are due to a strong decrease in both records since 1980 because of a short-term abrupt summer temperature decrease.

All temperature proxy records show exceptional high values in the last 20 years. This is not the case for the ice core δ^{18}O based temperature reconstruction, indicating a possible influence of melt water on the δ^{18}O record in this time (Fig. 5b).

δ^{18}O of cellulose chronology shows a highly significant opposite trend to δ^{18}O in the ice core that could be explained by the mixed signals of water sources (e.g. ground water, precipitation) and the influence of atmospheric circulation recorded in δ^{18}O of cellulose. The dramatic annual temperature increase showed by (Eichler et al. 2009) for the last 150 years is confirmed by thawing of the permafrost at our study site that is reflected in δ^{18}O of cellulose chronology.

4.3 Long-term variations in precipitation proxy records

The long-term trend in δ^{18}O of cellulose is well correlated with a precipitation reconstruction from Teletskoe lake sediments (Kalugin et al. 2007). This is not the case for MXD and δ^{13}C (Fig. 6a; Table 2). Precipitation records from lake Teletskoe and δ^{18}O in cellulose (Fig. 6b) show a clear increasing trend since the mid—nineteenth century. Based on the weather station data from Kosh-Agach the amount of winter precipitation since 1980 has decreased by up to 16 mm, while summer precipitation increased by up to 35 mm for the period 1934–1979. According to instrumental observations from the Barnaul weather station the sum of annual precipitation decreased from 650 to 450 mm/year for the period from 1900 to 2000. Earlier studies (Kalugin et al. 2007) show that the lack of changes in precipitation records could be due to extra-melting of perennial snow in high mountains before the background of an aridization trend.

The declining trend for the oxygen isotope ratio could be the result of (1) an increase in relative humidity during the studied period. With increasing air humidity the transpiration will be reduced because the gradient between the vapor pressure in the substomatal cavities and the ambient air decreases. As water molecules diffuse in both ways, out from the leaf to the atmosphere and vice versa, increasingly more water molecules (more depleted in ^{18}O than the leaf water) will diffuse back from the atmosphere into the leaf and reduce the leaf water enrichment. (2) With increasing annual temperatures in the recent years the permafrost, thaws more rapidly and deeper. A deeper thawing depth of the permafrost enhances the rooting depth, allowing the access to deeper and more ^{18}O depleted soil water, which is used for the synthesis of biomass. (3) We found good evidence that the oxygen isotope ratio in cellulose indicates climatic driven changes. These could include changes in the isotope signal of the precipitation (altering the δ^{18}O of the source water) driven by changes in atmospheric circulation and precipitation seasonality (as observed for other regions of northern Eurasia), but age trends in δ^{18}O of tree-rings cannot be ruled out completely (Treydte et al. 2006; Esper et al. 2010 submitted).

4.4 Uncertainties in multi-proxy data

In the year-to-year variability a multi-proxy data set consisting of tree-ring width, latewood density, cell wall thickness, δ^{13}C and δ^{18}O in cellulose chronologies agreed well with each other, while long-term climate information is recorded differently. This was observed in particular for oxygen isotopes in tree-rings, where the inter-annual variability was similar to the other parameters, while the long-term trends in smoothed chronologies were opposite.

This highlights a common difficulty of climate reconstructions from various archives, where often not all frequencies can be reconstructed with the same confidence. A well investigated problem, for instance, is the difficulty to obtain long-term climate variability from tree-ring width, because corrections of the age-trend may blur the climate information. The RCS-method (Briffa et al. 1996), which is often applied for keeping the long-term climatic signal (Naurzbaev et al. 2002; Esper et al. 2002; Sidorova 2003; Grudd 2008) in tree-ring width chronologies, is not always suitable. The cambial age and number of trees should be taken into account (Grudd 2008). The differences between high- and low-frequency information in δ^{18}O could be explained by the combined influence of different climate parameters, different seasonality and different response patterns to annual temperature and precipitation, which are significantly recorded in long-term annual signals rather than in the inter-annual variability. The diverging trends in δ^{18}O of cellulose and ice core further indicate that not only δ^{18}O of precipitation is determining δ^{18}O of tree-rings, but also plant-internal fractionations, which can be $H_2^{18}O$ enrichment in the leaf - governed by air humidity and transpiration or biochemical fractionations.

5 Conclusions

The reconstruction based on one proxy only could have uncertainties for the recent calibration period due to simultaneous temperature and CO_2 changes. The combination of TRW and δ^{13}C of cellulose proxies with ice core and lake sediment data will be beneficial for a temperature reconstruction. Our data verify the exceptionally strong temperature increase that occurred in this continental region during the last century.

Regarding precipitation, it is well known that it is difficult to build reconstructions, apart from arid regions, especially for sites where the signal could be masked by other factors. However, despite of the numerous factors influencing the δ^{18}O signal, our long-term tree-ring oxygen data agree well with the precipitation reconstruction from the Teletskoe lake sediments, which is a valuable contribution for improving our knowledge about the moisture regime in the Altai-Sayan region.

It is evident that the combination of several independent proxies improves the reliability and quality of the temperature and precipitation reconstructions back into past and will enhance our understanding of climate variations and facilitate more realistic predictions of possible vegetation shifts in Boreal forests.

Acknowledgments This work was supported by Swiss National Science Foundation SNF 200021_121838/1, Marie Curie International Incoming Fellowship (EU-ISOTREC 235122) awarded to the lead author, SCOPES Iz73z0-128035/1, RFBR no. 08-06-00253-a, RFBR no. 09-05-98015_r_sibir, AVZP Project 2.1.1/6131, Integration project SB RAS No 92, Scientific school (65610.2010.4). We are grateful to Jan Esper and Anne Verstege from WSL, Birmensdorf, Switzerland for providing access to the equipment for tree-ring cross-dating.

References

Adamenko MF (1978) Dynamics of larch tree growth as indicator of thermical regimes of summer in the Altai Mountain. Regional geographical investigations in the Western Siberia. Novosibirsk, Nauka, pp 20–23 (in Russian)

Alpatev AM, Arkhangelskiy AM, Podoplelov NY, Stepanov AY (1976) Physical geography of USSR: Asian part, Moscow (in Russian)

Ammann CM, Wahl ER (2007) The importance of the geophysical context in statistical evaluations of climate reconstruction procedures. Climatic Change 85:71–88. doi:10.1007/s10584-007-9276-x

Barber VA, Juday GP, Finney B (2000) Reduced growth of Alaskan white spruce in the twentieth century from temperature-induced drought stress. Nature 405:668–673

Blackman RB, Tukey J (1958) The measurement of power spectra. Dover, New York

Boettger T, Haupt M, Knöller K, Weise SM, Waterhouse JS et al (2007) Wood cellulose preparation methods and mass spectrometric analyses of δ^{13}C, δ^{18}O, and non exchangeable 2H values in cellulose, sugar and starch: an interlaboratory comparison. Anal Chem 79:4603–4612

Bradley RS (1999) Paleoclimatology. Reconstructing climate of the quaternary. Int Geophys Ser 64:613 p

Briffa KR, Jones PD, Schweingruber FH, Karlen W, Shiyatov SG (1996) Tree-ring variables as proxy indicators: problems with low-frequency signals. In: Climate change and forcing mechanisms of the last 2000 years, vol 141. Springer, Berlin, pp 9–41

Briffa K, Schweingruber F, Jones P, Osborn T (1998) Reduced sensitivity of recent tree growth to temperature at high northern latitudes. Nature 391:678–682

Cook ER, Kairiukstis LA (eds) (1990) Methods of dendrochronology. Applications in the environmental sciences. Kluwer Acad. Publ, Dordrecht, Boston, London, p 394 p

Cook ER, Krusic PJ (2008) A tree-ring standardization program based on detrending and autoregressive time series modeling, with interactive graphics (ARSTAN)

Craig H (1961) Isotopic variations in meteoric waters. Science 133:1702–1703

D'Arrigo R, Wilson R, Liepert B, Cherubini P (2008) On the "divergence problem" in northern forests: a review of the tree-ring evidence and possible causes. Global Planet Change 60:289–305

Dansgaard W (1964) Stable isotopes in precipitation. Tellus 16:436–468

Efimtsev NA (1958) Climatic studies. In: Proceeding of the Tuva multipurpose expedition: environment of the Tuva autonomous region, vol 3. AS USSR Press, Moscow, pp 46–65 (in Russian)

Eichler A, Oliver S, Henderson K, Laube A, Beer J, Papina T, Gäggeler HW, Schwikowski M (2009) Temperature response in the Altai region lags solar forcing. Geophys Res Lett 36:L01808. doi:10.1029/2008GL035930

Esper J, Cook ER, Schweingruber FH (2002) Low-frequency signals in long tree-ring chronologies and the reconstruction of past temperature variability. Science 295:2250–2253

Esper J, Frank DC, Battipaglia G, Büntgen U, Holert C, Siegwolf R, Saurer M (2010) Low frequency signals in tree-ring stable isotopes. Global Biogeochem Cycles (submitted)

Etien N, Daux V, Masson-Delmotte V, Mestre O, Stievenard M, Guillemin MT, Boettger T, Breda N, Haupt M, Perraud PP (2009) Summer maximum temperature in northern France over the past century: instrumental data versus multiple proxies (tree-ring isotopes, grape harvest dates and forest fires. Clim Change 94:429–456

Farquhar GD, Ehleringer JR, Hubick KT (1989) Carbon isotope discrimination and photosynthesis. Ann Rev Plant Physiol Plant Mol Biol 40:503–537

Francey RJ, Allison CE, Etheridge DM (1999) A 1000-year high precision record of δ^{13}C in atmospheric CO_2. Tellus B 51:170–193

Gagen M, McCarrolll D, Edouard J-L (2006) Combining tree-ring width, density and stable carbon isotope series to enhance the climate signal in tree-rings: and example from the French Alps. Climatic Change. doi:10.1007/s10584-006-9097-3

Gagen MH, McCarrol D, Robertson I, Loader NJ, Jalkanen R (2008) Do tree-ring δ^{13}C series from *Pinus sylvestris* in northern Fennoscandia contain long-term non-climatic trends? Chem Geol 252:42–51

Grudd H (2008) Torneträsk tree-ring width and sensitz AD 500–2004: a test of climatic sensitivity and a new 1500-year reconstruction of north Fennoscandian summers. Clim Dyn 31:843–857. doi:10.1007/s00382-007-0358-2

Helle G, Schleser GH (2004) Beyond CO2-fixation by rubisco—an interpretation of 13C/12C variations in tree rings from novel intra-seasonal studies on broad-leaf trees. Plant. Cell Environ 27(3):367–380

Henderson K, Laube A, Gäggeler HW, Olivier S, Papina T, Schwikowski M (2006) Temporal variations of accumulation and temperature during the past two centuries from Belukha ice core, Siberian Altai. Geophys Res 1:11. doi:10.1029/2005JD005819

Hilasvuori E, Berninger F, Sonninen E, Tuomenvirta H and Jungner H (2009) Stability of climate signal in carbon and oxygen isotope records and ring width from Scots pine (*Pinus sylvestris* L.) in Finland. Quat Sci 24(5):469–480

Ilyashuk BP, Ilyshuk EA (2007) Chironomid record of late quaternary climatic and environmental changes from two sites in Central Asia (Tuva Republic, Russia)—local, regional or global causes? Quat Sci Rev 26:705–731

Jones PD, Briffa KR, Barnett TP, Tett SFB (1998) High-resolution palaeoclimatic records for the last millennium: interpretation, integration and comparison with general circulation model control-run temperatures. Holocene 8:455–471

Kalugin I, Daryin A, Smolyaninova L, Andreev A, Diekmann B, Khlystov O (2007) 800-yr-long records of annual air temperature and precipitation over southern Siberia inferred from Teletskoye lake sediments. Quat Res 67:400–410

Kirdyanov AV, Treydte KS, Nikolaev A, Helle G, Schleser GH (2008) Climate signals in tree-ring width, density and ^{13}C from larch in Eastern Siberia (Russia). Cem Geol 252:31–41

Kress A (2009) Stable isotope dendroclimatology in the Swiss Alps: a 1200-year record from European larch. Dissertation ETH No. 18535, 113 p

Loader NJ, Switsur VR, Field EM, Carter AHC (1995) High resolution stable isotope analysis of tree rings: implications of microdendroclimatology for palaeoenvironmental research. Holocene 1(5):457–460

Loader NJ, Robertson I, Barker AC, Switsur VR, Waterhouse JS (1997) Improved technique for the batch processing of small whole wood samples to alpha-cellulose. Chem Geol 136:313–317

Loader NJ, Helle G, Los S, Lehmkuhl F, Schleser GH (2010) Twentieth-century summer temperature variability in the southern Altai Mountains: A carbon and oxygen isotope study of tree-rings. Holocene. doi:10.1177/0959683610369507

Mann ME and Jones PD (2003) Global Surface Temperatures over the Past Two Millennia GRL Vol. 3, N 15, 1820. doi:10.1029/2003GL017814

Mann ME, Bradley RS, Hughes MK (1998) Global-scale temperature patterns and climate forcing over the past six centuries. Nature 392:779–787

Mann M, Zhang Z, Hughes MK, Bradley RS, Miller SH, Rutherford S, Ni F (2008) Proxy-based reconstructions of hemispheric and global surface temperature variations over the past two millennia. Proc Natl Acad Sci 105(36):13252–13257. doi:10.1073/pnas.0805721105

McCarroll D, Loader NJ (2004) Stable isotopes in tree-rings. Quat Sci Rev 23:771–801

McCarroll D, Gagen MH, Loader NJ, Robertson I, Anchukaitis KJ, Los S, Young G, Jalkanen R, Kirchhefer A, Waterhouse JS (2009) Correction of tree-ring stable carbon isotope chronologies for changes in the carbon dioxide content of the atmosphere. Geochimica et Cosmochimica Acta. doi:10.1016/j.ca.2008.11.041

Myglan VS, Oidupaa OCh, Kirdyanov AV, Vaganov EA (2008) 1929-year tree-ring chronology for Altai-Sayan region (Western Tuva). J Archeol Ethnogr Anthropol 4(36):25–31 (in Russian)

Myglan VS, Ovchinnikov DV, Vaganov EA, Bykov NI, Gerasimova OV, Sidorova OV, Silkin PP (2009) Construction of 1772-year tree-ring width chronology for Altai Republic. Izvestiya RAN Serija Geograficheskaja 6:70–77 (in Russian)

Naurzbaev MM, Vaganov EA, Sidorova OV, Schweingruber FH (2002) Summer temperatures in eastern Taimyr inferred from a 2427-year late-Holocene tree-ring chronology and earlier floating series. Holocene 12(6):727–736

Nye JF (1963) Correction factor for accumulation measured by the thickness of the annual layers in ice sheets. J Glaciol 4(36): 785–788

Oidupaa OC, Vaganov EA, Naurzbaev MM (2004) Long-term summer temperature changes and tree radial growth of larch from the upper tree linein Altai-Sayan region. Lesovedenie 6:14–24 (in Russian)

Ovchinnikov DV, Panushkina IP, Adamenko MF (2002) Millennial tree-ring chronology of larch from the Altai Mountain and application for temperature reconstruction. Geogr Nat Resour 1:102–108

Panushkina IP, Ovchinnikov DV, Adamenko MF (2005) Mixed response of decadal variability in larch tree-ring chronologies from upper tree-lines of the Russian Altai. Tree Ring Res 61(1):33–42. doi:10.3959/1536-1098-61.1.33

Robertson I, Froyd CA, Gagen M, Hicks S (2009) Climates of the past: evidence from natural and documentary archives. J Quat Sci 24(5):411–414

Saurer M, Siegwolf RTW (2007) Human impacts on tree-ring growth reconstructed from stable isotopes. In: Dawson TE, Siegwolf RTW (eds) Stable isotopes as indicators of ecological change. Terrestrial ecology series. Elsevier, Amsterdam, Boston, pp 49–62

Saurer M, Borella S, Schweingruber F, Siegwolf R (1997) Stable isotopes in tree-rings of beech: climatic versus site-related influences. Trees 11:291–297

Saurer M, Robertson I, Siegwolf R, Leuenberger M (1998) Oxygen isotope analysis of cellulose: an interlaboratory comparison. Anal Chem 70:2074–2080

Saurer M, Schweingruber F, Vaganov EA, Schiyatov SG, Siegwolf R (2002) Spatial and temporal oxygen isotope trends at the northern tree-line in Eurasia. Geophys Res Letts 29(9). doi:10.1029/2001GL013739

Schweingruber FH (1996) Tree-rings and environment dendroecology. Paul Haupt Publ, Bern, Stuttgart, Vienna, p 609 pp

Schweingruber FH, Karlen W, Shiyatov SG (1996) Tree-ring variables as proxy indicators: problems with low-frequency signals. Climate change and forcing mechanisms of the last 2000 years. NATO ASI Series, vol 141. Springer, Berlin, pp 9–41

Selegei V, Dehandschutter B, Klerkx J, Vysotsky E (2001) The physical and geological environment of lake Teletskoye. Royal museum of central Africa, Tervuren, Belgium. Ann Sci Geol 105:310

Sevastyanov VV (1998) Climate of high altitude Altai and Sayan region. Tomsk, 202 p (in Russian)

Sidorova OV (2003) Long-term climatic changes and the larch radial growth on the northern Middle Siberia and the North-Eastern Yakutia in the Late Holocene. Abs. of PhD dissertation, 2003, 18 p (in Russian)

Sidorova OV, Siegwolf RTW, Saurer MM, Naurzbaev MM, Vaganov EA (2008) Isotopic composition (δ^{13}C, δ^{18}O) in Siberian tree-ring chronology. Geophys Res Biogeo 113:G02019. doi:10.1029/2007JG000473

Sidorova OV, Siegwolf RTW, Saurer M, Shashkin AV, Knorre AA, Prokushkin AS, Vaganov EA, Kirdyanov AA (2009) Do centennial tree-ring and stable isotope trends of Larix gmelinii (Rupr.) Rupr. indicate increasing water shortage in the Siberian north? Oecologia 161:825–835. doi:10.1007/s00442-009-1411-0

Sidorova OV, Siegwolf RTW, Saurer MM, Naurzbaev MM, Shashkin AV, Vaganov EA (2010) Spatial patterns of climatic changes in the Eurasian north reflected in Siberian larch tree-ring parameters and stable isotopes. Global Change Biol 16:1003–1018. doi:10.1111/j.1365-2486.2009.02008.x

Skomarkova MV, Vaganov EA, Mund M, Knohl A, Linke P, Boerner A, Schulze E-D (2006) Inter-annual and seasonal variability of radial growth, wood density and carbon isotope ratios in tree-rings of beech (*Fagus sylvatica*) growing in Germany and Italy. Trees 20:571–586

Treydte K, Schleser GH, Helle G, Winiger M, Frank DC, Haug GH, Esper J (2006) The twentieth century was the wettest period in northern Pakistan over the past millennium. Nature 440:1179–1182

Vaganov EA, Hughes MK, Kirdyanov AV, Schweingruber F, Silkin PP (1999) Influence of snowfall and melt timing on tree growth in Subarctic Eurasia. Nature 400:149–151

Vaganov EA, Hughes MK, Shashkin AV (2006) Growth dynamics of tree-rings: an image of past and future environments. Springer, New York 354 p

Wigley T, Briffa K, Jones P (1984) On the average value of correlated time series, with application in dendroclimatology and hydrometeorology. J Clim Appl Met 23:201–213

Wilmking M, D'Arrigo R, Jacoby G, Juday G (2005) Divergent growth responses in circumpolar boreal forests. Geophys Res Lett 32:L15715. doi:10.1029/2005GLO23331